Subchronic phencyclidine (PCP) treatment produces schizophrenia-like alterations in functional integration and brain network structure in rats

Neil Dawson[1,2,3], Xiaolin Xiao[4], Des Higham[3,4], Brian Morris[1,5], Judith Pratt[1,2,3]

1. Psychiatric Research Institute of Neuroscience in Glasgow (PsyRING), Glasgow, G12 8QQ, UK. 2. Strathclyde Institute of Pharmacy and Biomedical Sciences, University of Strathclyde, G4 0RE, UK 3. Centre for Neuroscience, University of Strathclyde (CeNsUS), G4 0RE, UK. 4. Department of Mathematics, University of Strathclyde, G11 1XH, UK. 5. Institute of Neuroscience and Psychology, University of Glasgow, G12 8QQ, UK.

Email: neil.dawson@strath.ac.uk   www.psyring.co.uk

Introduction

• Compromised functional integration between neural systems is hypothesised to contribute to the cognitive deficits seen in schizophrenia.

•Functional interactions between discrete brain regions can be represented as a complex network of nodes (regions) linked by edges with defined association strengths (weights). The properties of functional brain networks can be quantified through the application of complex network analysis, largely based on graph theory (see Bullmore and Sporns, 2009 for a brief overview).

• Here we apply these analytical methods to characterise network structure in functional brain networks derived from ^{14}C-2-deoxyglucose autoradiographic imaging data gained from control animals and those treated subchronically with the NMDA receptor antagonist Phencyclidine (PCP). The PCP treatment regime used in this study induces cognitive deficits, neurochemical and molecular alterations and alterations in overt cerebral metabolism (including "hypofrontality") that parallel those seen in schizophrenia (Pratt et al., 2008) .

Methods

• Cerebral metabolism in 64 discrete RoI was determined in control animals (saline, male, Lister Hooded, n=7) and rats treated subchronically with PCP (2.58mg.kg^{-1}, *i.p.*, 1x daily for 5 days) by semi-quantitative 2-deoxyglucose autoradiography (Dawson et al., 2009) 72 hours after the final treatment.

• Functional connectivity brain networks for each experimental group were generated as binary adjacency matrices over a range of correlation thresholds (Pearson's correlation co-efficient 0.4 to 0.5) from the inter-regional partial correlation matrices (Fishers z-transformed) derived from 2-deoxyglucose data. Graph theoretical analysis was used to quantitatively define the topological properties of the functional brain network in each experimental group.

• Global network properties were characterised in terms of mean degree (<k>), average path length (Lp), mean clustering co-efficient (Cp) at each correlation threshold (T).

• Centrality analysis (degree, betweeness and closeness) was used to identify brain regions which act as hubs in the functional brain networks.

• To determine potential alterations in the functional integrity of specific neural systems regional clustering that was exclusive to one of the two experimental treatment groups was determined through the application of a novel algorithm based upon the Generalized Singular Value Decomposition (GSVD) (Xiao et al., 2010).

Statistics

Overt alterations in regional were analysed using t-test. Differences in global network architecture between experimental groups were analysed using repeated measures ANOVA. Hub regions were identified by statistically comparing real with calibrated random (Erdös-Renyi) graphs. Alterations in regional centrality between groups were analysed by comparing regional z-scores, generated relative to random graphs, using t-test with Bonferroni correction. The exclusivity of regional clustering to an experimental group was determined by the calculation of a clustering quality measure in the GSVD reordered matrices relative to 1000 random permutations. Significant over-abundance of a given neural system in a GSVD defined cluster was determined by hypergeometric probability with Bonferroni correction. Significance was set at p<0.05 throughout.

References

Bullmore and Sporns, 2009. Nat. Rev. Neurosci. 10: 186. Dawson et al., 2009. J. Neuro. Res. 87: 2375. Liu et al., 2008. Brain. 131: 945. Micheloyannis et al., 2006. Schizophr. Res. 87: 60. Pratt et al., 2008. Br. J. Pharmacol. 153: S465. Xiao et al., 2010. BMC Systems Biology (submitted)

Acknowledgements

PsyRING is a collaborative venture between the Universities of Glasgow and Strathclyde and NHS Greater Glasgow and Clyde.
This work was funded by the EPSRC Bridging the Gap funded program at the University of Strathclyde.

Results

Subchronic PCP treatment induces overt hypofrontality and thalamic hypometabolism

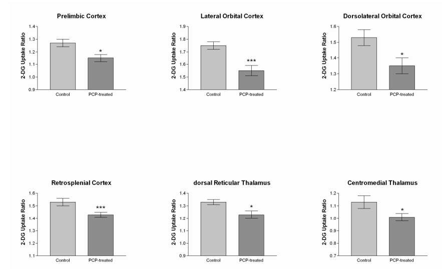

Subchronic PCP treatment induces significant overt hypometabolism in discrete regions of the prefrontal cortex and thalamus. *denotes p<0.05 and ***denotes p<0.001 significant difference from control (t-test).

Subchronic PCP-induced alterations in global network properties

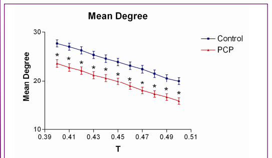

Subchronic PCP treatment results in a significant decrease in the average number of connections (mean degree, <k>) in the functional brain network at all thresholds. PCP-treated animals significantly different from controls across all thresholds (p<0.001, $F_{(1,21)}$= 1178 repeated measures ANOVA) and at each independent threshold level (*denotes p<0.05, t-test with Bonferroni correction).

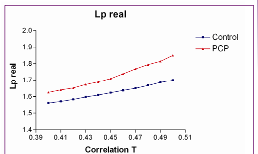

The average path length (L_p), across all correlation thresholds, is significantly increased in the functional brain network of PCP-treated animals (p<0.001, $F_{(1,21)}$= 197.191 repeated measures ANOVA). Shortest absolute path length is the minimum number of edges (connections) in the network that must be traversed to go from one node (RoI) to another. The average path length is the average of these shortest paths between all nodes in the network. A low average path length is indicative of a network allowing efficient information transfer between nodes.

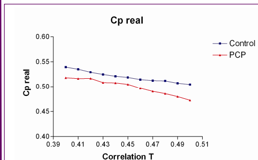

Brain regions in the functional brain network of PCP-treated animals show reduced clustering in comparison to the network in control animals. The clustering co-efficient (C_p real) is significantly reduced, across all correlation thresholds, in PCP-treated animals relative to controls (p<0.001, F $_{(1,21)}$ = 185.442, repeated measures ANOVA). This suggests that information transfer between neighbouring nodes, present in the control network, is impeded in the PCP treated animals.

The identity of hub brain regions in the functional brain network is altered in PCP-treated animals

Table 1. Hub regions lost in PCP-treated animals

Region	Degree Z-score	Degree p-value	Betweeness Z-score	Betweeness p-value	Closeness Z-score	Closeness p-value
Retrosplenial Cortex (RSC)	-0.04	2.786	**3.47**	**0.000**	0.57	**0.933**
Nucleus accumbens core (NacC)	0.72	0.316	**3.22**	**0.000**	1.98	**0.004**
dorsal Reticular Thalamus (dRT)	**11.26**	**0.000**	**5.81**	**0.000**	**6.14**	**0.000**
ventral Reticular Thalamus (vRT)	**8.48**	**0.000**	**3.65**	**0.000**	**4.39**	**0.000**
Mediodorsal Thalamus (MDthal)	0.99	0.141	**5.72**	**0.000**	1.52	**0.019**
Centrolateral Thalamus (CLthal)	**3.06**	**0.000**	**4.95**	**0.000**	**3.05**	**0.000**
Ventrolateral Thalamus (VLthal)	**2.89**	**0.000**	**6.41**	**0.000**	2.28	**0.001**
Nucleus Reuniens (Re)	**5.40**	**0.000**	**12.87**	**0.000**	**4.68**	**0.000**
Hippocampus CA2	**23.39**	**0.000**	**4.14**	**0.000**	**6.84**	**0.000**
Lateral Habenula (lHab)	1.63	0.318	**4.75**	**0.000**	1.88	**0.004**
Locus Coeruleus (LC)	**9.79**	**0.000**	**8.16**	**0.000**	**6.72**	**0.000**

Table 2. Hub regions gained in PCP-treated animals

Region	Degree Z-score	Degree p-value	Betweeness Z-score	Betweeness p-value	Closeness Z-score	Closeness p-value
Frontal Association Cortex (FRA)	**-3.922**	**0.000**	**-3.804**	**0.000**	-1.965	**0.002**
Prelimbic Cortex (PrL)	-1.029	0.085	-2.388	**0.005**	-1.551	**0.022**
Lateral Orbital Cortex (LO)	**-3.146**	**0.000**	**-4.811**	**0.000**	**-4.894**	**0.000**
Dorsolateral Striatum (DLST)	**-3.952**	**0.000**	-2.326	**0.006**	**-4.551**	**0.000**
Bed Nucleus of the Stria Terminals (BNST)	**-2.448**	**0.000**	**-5.324**	**0.000**	-0.255	1.660
Anteroventral Thalamus (AVthal)	**-3.334**	**0.000**	**-3.444**	**0.000**	**-2.772**	**0.000**
Rhomboid Nucleus (Rh)	-0.186	2.013	**-3.413**	**0.000**	-0.589	0.733
Medial Habenular (mHab)	**-3.905**	**0.000**	**-5.079**	**0.000**	-2.482	**0.002**
Piriform Cortex (Piri)	-2.427	**0.000**	**-3.891**	**0.000**	**-2.898**	**0.000**
Hippocampal Subiculum (Sub)	**-3.983**	**0.000**	**-5.382**	**0.000**	**-4.560**	**0.000**
Interpeduncular Nucleus (IP)	**-3.445**	**0.000**	**-7.595**	**0.000**	-2.303	0.066

Tables 1 and 2. Hub regions lost and gained in PCP-treated animals. Within each centrality measure (degree, betweeness and closeness) the centrality of a given region was considered to be significantly altered if the z-score difference between PCP-treated and control animals for a given brain region was >2.576 and p<0.05 (t-test with Bonferroni correction). Bold denotes values which meet this criteria. Regions highlighted in red denote regions where centrality is significantly altered across all measures.

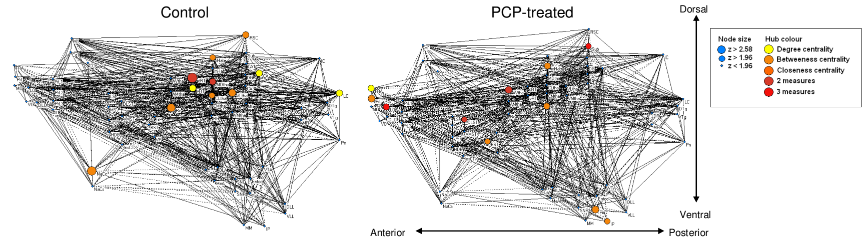

Hub regions in the Control Network
• Locus Coeruleus (LC)
• dorsal Reticular Thalamus (dRT)
• ventral Reticular Thalamus (vRT)
• Ventrolateral Thalamus (VLthal)
• Centrolateral Thalamus (CLthal)
• Mediodorsal Thalamus (MDthal)
• Nucleus Reuniens (Re)
• Retrosplenial Cortex (RSC)
• CA2 subfield of the Hippocampus (CA2)
• Nucleus accumbens core (NacC)
• Lateral Habenula (lHab)

Hub regions in the PCP Network
• Frontal Association Cortex (FRA)
• Prelimbic Cortex (PrL)
• Lateral Orbital Cortex (LO)
• Dorsolateral Striatum (DLST)
• Bed Nucleus of the Stria Terminals (BST)
• Anteroventral Thalamus (AVthal)
• Medial Habenula (mHab)
• Rhomboid Nucleus (Rh)
• Dorsal Subiculum (Sub)
• Piriform Cortex (Piri)
• Interpeduncular Nucleus (IP)

Figure showing important hub regions in the functional brain network of control animals and those treated with subchronic PCP. Brain regions, represented as nodes, are situated according to their anterior-posterior and dorsal-ventral anatomical location. Hub brain regions were identified relative to calibrated random (Erdos-Renyi) graphs. Only those regions with a standardized z-score >1.96 in the real relative to the random network in any centrality measure were identified as important hubs. Node size reflects the standardized z-score of each region. Regions are colour coded on the basis of the centrality measures in which they were identified as important hubs. Solid lines represent a positive functional correlation between regions whereas dashed lines represent a negative functional correlation between brain regions. Networks are shown at the threshold T=0.5.

The functional clustering of neural systems is altered in PCP-treated animals

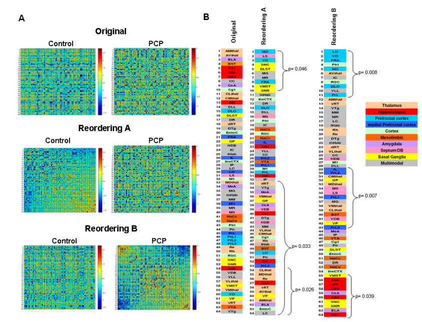

Figure showing GSVD identified differences in regional clustering between the two experimental groups. (A) Heatmaps showing the functional clustering of brain regions exclusive to control (reordering A) and PCP-treated (reordering B) animals. Visually there appear to be 1 cluster exclusive to control animals and 3 clusters exclusive to PCP-treated animals. (B) Brain region lists showing the ordering of brain regions in the original and GSVD reordered brain matrices. In both reordering A (control exclusive) and reordering B (PCP exclusive) 3 significant clusters were identified by comparison of the cluster quality measure in the real matrices as compared with 1,000 random permutations. When brain regions are colour coded on the basis of the neural systems in which they function, there appears to be an over-abundance of specific neural systems in the GSVD identified clusters.

Table 3. Neural system over-representation in GSVD identified functional clusters

Reordering	Cluster	Cluster p-value	Cluster size	Neural System	Regions in Subsystem (*N*)	Regions in Cluster (n)	hypergeometric probability P(X ≥ n)
A	nodes 1-10	0.046	10	Basal Ganglia	6	4	4.192×10^{-3}
	nodes 33-64	0.033	32	Thalamus	11	11	1.735×10^{-4}
	nodes 54-64	0.026	11	Thalamus	11	6	1.918×10^{-3}
				Control Hubs	12	6	3.532×10^{-3}
B	nodes 1-11	0.008	11	Prefrontal Cortex	6	6	6.162×10^{-6}
	nodes 29-43	0.007	14	medial Prefrontal cortex	4	4	1.575×10^{-3}
	nodes 55-64	0.039	10	Hippocampus	5	5	3.305×10^{-5}

Table 1. Specific neural subsystems are significantly overrepresented in the GSVD identified functional clusters exclusive to one experimental group. Criteria for the significant over-abundance of a given neural system was set at a hypergeometric probability of P(x≥n)<0.005 (Bonferroni corrected for multiple comparisons). Regions of the Basal Ganglia and Thalamus were functionally clustering in control but not PCP-treated animals. In PCP-treated animals the Prefrontal Cortex, medial Prefrontal Cortex and Hippocampus form discrete functional clusters that are not present in controls.

Conclusions

• PCP-induced alterations in the global topology of the functional brain network, including decreased mean degree (<k>), increased average path length (L_p), decreased clustering coefficient (C_p) parallel those reported in functional brain networks in schizophrenia (Liu et al., 2008; Micheloyannis et al., 2006). PCP-induced alterations in the global topology of the functional brain network are indicative of reduced connectivity resulting in reduced network efficiency for information transfer, both across the entire network (Lp) and at a local level (Cp).

• The loss of multiple thalamic regions (dRT, vRT, CLthal, Re) as hub brain regions in the network of PCP-treated animals may contribute to the reduced efficiency of this network. These results support the hypothesis of disrupted thalamic connectivity in schizophrenia.

• The loss of thalamic connectivity in PCP-treated animals results in compromised functional integration between the prefrontal cortex and hippocampus, as evidenced by the discrete clustering of these neural systems in PCP-treated but not control animals.

• Altered functional connectivity of the locus coeruleus (LC) supports a role for disrupted noradrenergic neurotransmission in PCP-treated animals and schizophrenia.

• The resemblance of PCP-induced alterations in brain network structure to those seen in schizophrenia further supports a role for glutamatergic disruption in this devastating disease.